The chemical and physical characteristics of single-walled carbon nanotube film impact on osteoblastic cell response

Wojtek Tutak[1]**, Manish Chhowalla**[1,3] **and Federico Sesti**[2,3]

[1] Materials Science and Engineering, School of Engineering Rutgers, State University of New Jersey, Piscataway, NJ 08854, USA
[2] Department of Physiology and Biophysics, University of Medicine and Dentistry of New Jersey-Robert Wood Johnson Medical School, Piscataway, NJ 08854, USA

E-mail: manish1@rci.rutgers.edu and sestife@umdnj.edu

Abstract

Carbon-nanotube-based substrates have been shown to support the growth of different cell types and, as such, have raised considerable interest in view of their possible use in biomedical applications. Nanotube matrices are embedded in polymers which cause inherent changes in nanotube chemical and physical film properties. Thus, it is critical to understand how the physical properties of the film affect the biology of the host tissue. Here, we investigated how the physical and chemical properties of single-walled carbon nanotubes (SWNT) films impact the response of MC3T3-E1 bone osteoblasts. We found that two fundamental steps in cell growth—initial attachment to the substrate and proliferation—are strongly dependent on, respectively, the energy and roughness of the surface. Thus, fine-tuning the properties of the film may represent a valid strategy to optimize the response of the biological host.

(Some figures in this article are in colour only in the electronic version)

1. Introduction

Numerous studies underscore the potential application of single-walled carbon nanotubes (SWNTs) in cell scaffolding [1, 2], cancer cell therapies [3] and drug delivery [4]. In an effort to develop efficient SWNT-based substrates able to support the growth of bone cells, we recently introduced a novel substrate constructed by depositing SWNTs onto multicellulose ester (MCE) membranes. These thin films promote the growth of primary rat calvariae osteoblastic cells and mouse preosteoblastic MC3T3-E1 cells by stimulating the production of an extracellular matrix, a central step in bone tissue formation [5]. SWNT films are especially attractive because they appear to be bio-inert, an important feature in view of their possible use in biomedical applications.

A crucial factor concerning SWNT-based substrates is that their physical and chemical characteristics vary depending on methods used to synthesize and purify the nanotubes [1]. In all cases, the nanotubes require post-synthesis processing in order to obtain reproducible, catalyst-and impurity-free product applicable in biological experiments. For example, purification performed in acids such as HCl [6], HNO$_3$ [7] or H$_2$SO$_4$ [8] can significantly alter the nanotube chemistry (side wall attachment of functional groups) and its size (tube cleavage) distribution. These modifications alter the attributes of the substrate, ultimately affecting the response of the biological host. Thus it is crucial to understand how the physical and chemical characteristics of SWNT films affect cell growth.

Here we show that two basic film parameters, namely the surface energy density and roughness, are key in modulating the growth of bone osteoblasts. Specifically the surface energy density is important in promoting the initial attachment of the cell to the substrate whereas surface morphology is crucial in supporting subsequent proliferation. Film surface energy and roughness can be controlled during the materials processing step. This implies that by controlling these quantities, it is possible to tailor SWNT films to optimize specific developmental steps during bone histogenesis.

---

[3] Authors to whom any correspondence should be addressed.

2. Experimental details

2.1. SWNT film preparation

Single-walled carbon nanotubes purchased from 'Unidym' were purified following a protocol reported by Xu *et al* [9]. Thus, the nanotubes were dispersed in water until a stable suspension was formed [10]. An aqueous dispersion of 8 μg ml^{-1} SWNTs and 1% (w/v) of sodium dedocylsulfate (SDS, Sigma Aldrich) was then ultrasonicated for 3 h. To eliminate agglomerated nanotubes the suspension was left to settle for 96 h [10]. Then, the nanotube suspension was deposited on filter mixed-cellulose ester membranes (MCE, Millipore). The carbon nanotube suspension was filtered using a vacuum filtration apparatus at constant suction power [11]. Specifically, 20, 35 and 50 ml of nanotube suspension were deposited onto 20, 220 and 800 μm pore size filter membranes. The amount of SWNT suspension deposited onto MCE membranes was experimentally optimized to form free-standing SWNT films using the minimum allowable amount. Carbon nanotube membranes were cut in circular size and MCE backing dissolved in a series of acetone baths. Free-floating SWNT films were then removed and placed on glass slides (Fisher Scientific), dried in an oven and maintained under UV light (254 nm) prior to their utilization.

2.2. Films functionalized with COOH groups

In order to verify our ability to control surface energy density, the nanotube film's chemistry was reversed by attaching COOH groups. The chemical treatment was performed according to a procedure outlined by Parekh *et al* [12]. Specifically, the carbon films were treated for 3 h in an azeotropic nitric acid bath (69.7% HNO$_3$) gently blown with nitrogen gas and vacuum-dried. Prior to surface measurements, the films were rinsed in deionized water (DI) and dried.

2.3. Surface characterization (SEM, AFM, surface energy density)

For surface morphology, roughness and surface energy density assessment, SWNT samples were rinsed in DI water, dried and blown gently with nitrogen gas. Samples selected for assessing surface morphology were coated with a 20 nm layer of gold and measured using a scanning electron microscope (SEM, Philips, XL 30 FEG). Surface roughness and surface area were assessed using an atomic force microscope (AFM; Nanoscope IIIa, Veeco, CA) in tapping mode on a 10 μm $\times$ 10 μm area. The surface roughness coefficient, R_q, was calculated as the root mean square of the height (h):

$$R_q = \sqrt{\frac{\sum_{j=1}^{N}\left(h_j\right)^2}{N}} \qquad (1)$$

where $\langle h \rangle$ is the average height and N is the sampling size.

A goniometer (Ramehart, model 200) was used to measure surface–liquid contact angles. Static contact angles varying from 30° to 130° were recorded 30 s after a drop ($\sim$15 μl) of phosphate buffered (PBS) solution or ethylene glycol was cast on the surface. Tests were repeated in triplicate. Surface energy density, φ, was calculated as the unitary surface tension (for a liquid these two quantities are identical):

$$\varphi = \gamma_s^d + \gamma_s^p \qquad (2)$$

where the solid dispersion and polar coefficients, γ_s^d and γ_s^p, were calculated by the Owens–Wendt function:

$$(\gamma_l^d + \gamma_l^p)\cos\theta = 2\left(\sqrt{\gamma_s^d\gamma_l^d} + \sqrt{\gamma_s^p\gamma_l^p}\right) - 1 \qquad (3)$$

where the surface tension coefficient γ_l^d and γ_l^p for PBS and ethylene glycol are, respectively, 0.22 and 35.2, and 0.29 and 19.0 mN m^{-1}.

2.4. Cell cultures

MC3T3-E1 osteoblastic cells plated at 5000 cells/well (1.6 cm) were supplemented with Eagle's minimal essential medium (α-MEM), 10% fetal bovine serum (FBS) and 1% pen-strep bactericide (PS). Cells were stained using Calcein AM fluorescent dye (Invitrogen), 1 h prior to rinsing with PBS. The cells were visualized under a 10$\times$ objective (Olympus) with 2.4 mm^2 field of view, on areas located on opposite sides of each sample. Corresponding cell density at days 1, 3 and 5 was calculated using Image J software.

2.5. Cell adhesion assay

Six hours after initial cell deposition, cells were stained with Calcein AM fluorescent dye. The cells were counted as described before (section 2.4) and then rinsed five times in 1 ml PBS at 2 min intervals (average calculated applied force $\sim$0.1 Pa). The cells remaining on the film were counted a second time compared to the initial cell number and expressed as a percentage of attached cells.

2.6. Statistical analysis

Quantitative data are presented as mean $\pm$ standard error of the mean (SEM). The level of significance was calculated using Student's t-test for single comparisons and ANOVA for multiple comparisons using a Tukey means comparison test with 95% confidence level. Statistical significance was assumed at the 95% confidence limit or greater ($P < 0.05$).

3. Results

In this study, we have utilized highly purified SWNT suspensions to deposit uniform carbon nanotube networks using vacuum filtration methods [12, 13]. This protocol allows us to control the thickness and roughness of the substrate. The resulting films have similar physical and chemical properties and therefore direct comparisons between networks with varying roughness and/or surface energy density (φ) can be made.

To control the morphology of the substrate we maintained the supporting membrane (MCE) under constant vacuum pressure while allowing the insertion of the nanotubes into
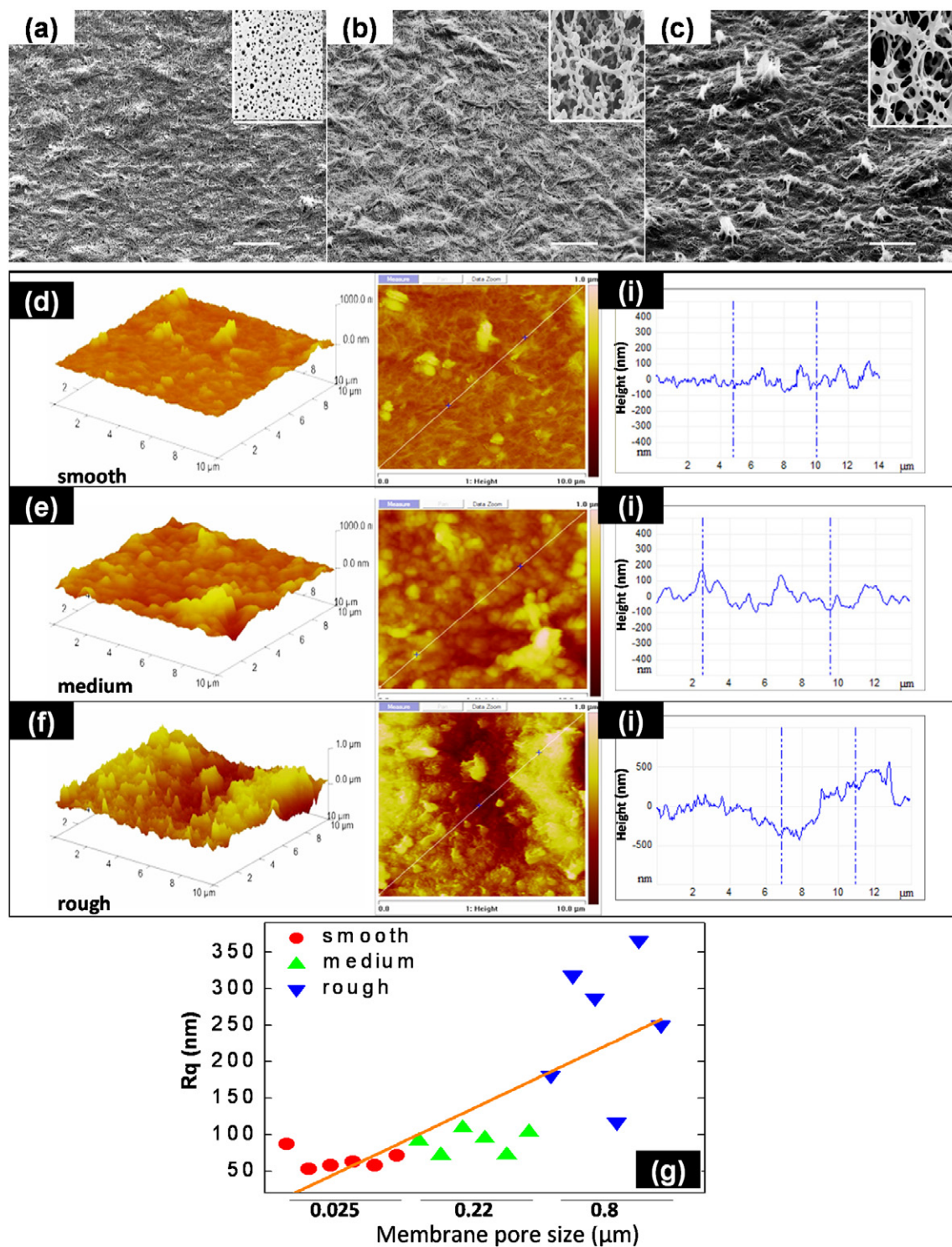
Figure 1. SWNT films vary in surface morphology. (a)–(c) Representative EM images of carbon nanotube films obtained with (left to right) filter membrane pore sizes (insets): 0.025, 0.22 and 0.8 μm, respectively. Scanning electron images were taken at $\times 10\,000$, scale mark at 2 μm. (d)–(f) Representative AFM digital images of the nanotube film surfaces shown in (a)–(c). In the insets d(i)–f(i) are shown typical cross-sectional areas of tested films showing variation in height, peak size and peak distribution. (g) Relationship between surface roughness and filter membrane pore size.

the pores of the membrane. Figures 1(a)–(c) show scanning electron images of the SWNT films and the corresponding MCE membranes (insets) with three different pore sizes (25, 220 and 800 nm, left to right). It appears that larger pores give rise to rougher surfaces. This qualitative impression

was confirmed by measuring the roughness coefficient (R_q, equation (1)) of the various films by means of atomic force microscopy (AMF) in tapping mode. Typical digitized AFM scans of the films are shown in figures 1(d)–(f), along with representative line scans showing the variation in height
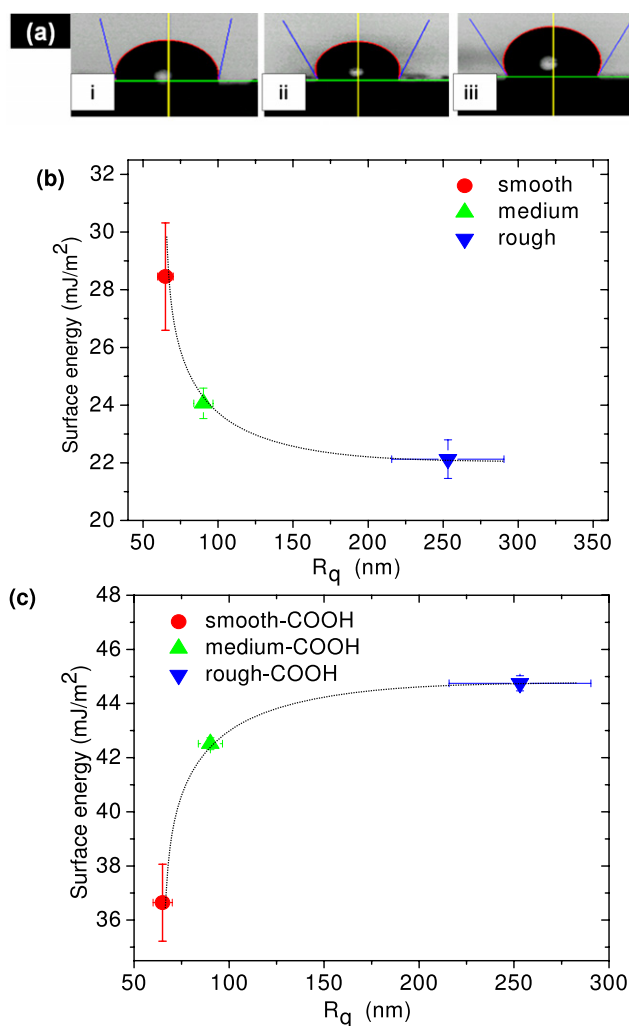
Figure 2. Chemical and physical characteristics of SWNT films. (a) Representative images of PBS sessile drops on (i) smooth, (ii) medium and (iii) rough films. (b) Relationship between surface energy density and surface roughness in pristine nanotube films. The line highlights the trend in film hydrophobicity ($n = 6$ experiments). (c) Relationship between surface energy density and surface roughness in SWNT-COOH films ($n = 6$ experiments).

(figures 1(d)(i)–f(i)). The calculated R_q values of the SWNT networks were 60.64 ± 12.38, 90.22 ± 15.58 and 253.41 ± 91.47 nm ($n = 6$ experiments) for, respectively, 25, 220 and 800 nm pore sizes, confirming the notion that there is a reasonable increase in network roughness with pore size (figure 1(g)).

To further investigate the basic properties of the SWNT networks, we measured their surface energy density (φ, equation (2)) using the contact angle formed between PBS and ethylene glycol (EG) sessile drops deposited on top of the films. Representative images of the drops on the various surfaces are illustrated in figure 2(a). Our results, presented in figure 2(b), show that for films constructed with pristine nanotubes, φ decreases with roughness. Pristine nanotubes are hydrophobic in nature and, on the other hand, φ is dependent on the hydropathy of the surface. However, pristine SWNTs can be turned hydrophilic by a mild treatment

with nitric acid (see the methods section) [12]. For carbon films functionalized with carboxyl groups (SWNT-COOH) φ increased with roughness (figure 2(c)). Specifically, at medium roughness ($R_q \sim 100$ nm) the extrapolated φ roughly doubled in hydrophilic SWNT-COOH films. Thus, φ in SWNT films can be controlled by surface chemistry and roughness.

Having characterized the physical and chemical properties of the SWNT films we focused on the impact of these parameters on biological cells. We used MC3T3-E1 osteoblastic cells in our experiments, which we previously showed to respond well to this type of substrate [5]. We initially investigated cell attachment to the substrate as a function of φ and roughness. To compare SWNT films before and after adhesion tests we developed the *ad hoc* sample design shown in figure 3(a). Cells were stained with Calcein AM fluorescent dye and counted. After thorough rinsing, the cells remaining on the film were counted a second time and compared to the initial cell number. The figure shows the regions investigated under an optical microscope, with the yellow squares corresponding to the SWNT networks. Bright light images are shown in inset (i) whereas the same areas under fluorescent light are shown in inset (ii). The results of cell attachment tests for the various film types are shown in figure 3(b). Observed cell attachment was significantly higher on hydrophilic than hydrophobic films, irrespective of their surface roughness. However, in both hydrophilic and hydrophobic films cell adhesion was maximal in medium roughness ($R_q \sim 100$ nm). Similar results were obtained using primary calvariae osteoblastic cells (data not shown). Representative images of cells taken 72 h after initial seeding on pristine nanotube films are shown in figures 3(c)–(e). Cells showed robust spreading on medium roughness networks (figure 3(d)). Filopodia and lamellipodia cytoplasmic digitations were noticeably present in these samples under fluorescent light. On the other hand, cells grown on the smooth and rough substrates showed less cytoplasmic extensions (figures 3(c)–(e)).

Together these data indicate that φ and, to a lesser extent, surface roughness play an important role in initial cell adhesion. Films constructed with hydrophilic nanotubes yielded better attachment than hydrophobic films even though the roughness was the same in both film types. However in both hydrophobic and hydrophilic films adhesion was maximal in medium roughness surfaces. Thus these observations suggest that surface roughness can further improve cell adhesion.

The cell to material response was further investigated by measuring cell proliferation within the first five days. The results of these experiments, carried out on both hydrophobic and hydrophilic films, are shown in figure 4. Proliferation was moderately improved in hydrophilic films. Most notably, proliferation was highest on smooth surfaces. This suggests that the roughness of the surface is the most important parameter in determining cell proliferation whereas φ appears to play only a marginal role.

In short, an optimized surface morphology in which φ is high and roughness is medium provide optimal conditions for these film types.
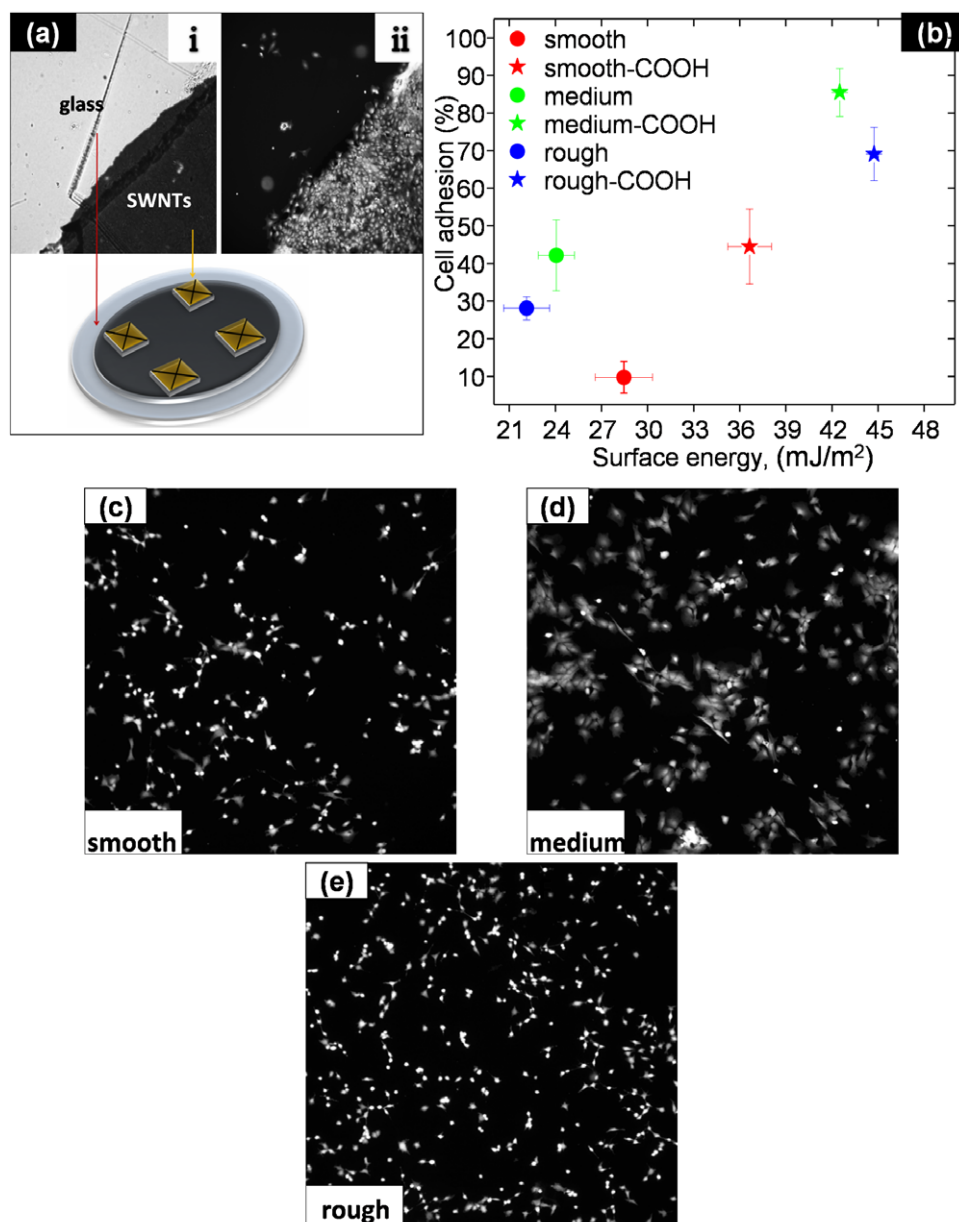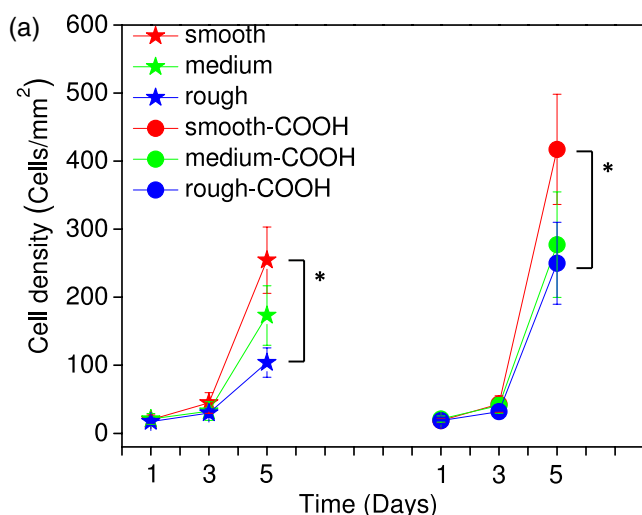
Figure 3. Surface energy density and surface roughness impact initial cell adhesion. (a) Typical sample set-up used in the experiments. The yellow crossed boxes correspond to carbon films viewed under a microscope (not to scale). Insets: the same areas (i) before and (ii) after cell seeding. Note that cells adhered on the SWNT film but not on the glass support. (b) Osteoblastic cells attachment as a function of the surface energy density of hydrophobic and hydrophilic films ($n \geqslant 6$). (c)–(e) Representative images showing cell's cytoplasmic extensions on the indicated pristine surfaces. Extensions are visibly larger on medium films indicating higher cell–material interaction.

4. Discussion

In this study we have investigated how the physical and chemical characteristics of SWNT-based films support the growth of MC3T3-E1 osteoblasts. We found that both the surface energy density and the roughness of the SWNT surface are key in determining the cell's response. Two fundamental cellular processes, adhesion and proliferation, were affected by these two quantities in a complementary fashion. Thus, φ was crucial in promoting cell attachment and played only a marginal role in subsequent proliferation. In contrast, surface roughness was key in proliferation and only marginal in initial adhesion. The reported high proliferation rates on smooth

nanotube films are expected, particularly when considering the dynamics of cell mitosis. However, it is not completely understood why initial cell attachment peaks for medium roughness surfaces and future studies will be needed to address this point.

Overall, wettable SWNT-COOH films exhibit the best growing conditions for MC3T3-E1 osteoblasts. It is likely that the high φ of these films, by promoting attachment and the development of cytoplasmic extensions, provides a growing advantage to cells that enhances their later development. A unique feature of SWNT films is that they can be hydrophobic and support cell growth, as the majority of bioactive materials commonly used for cell culturing is wettable [14]. Even though

Figure 4. Surface energy density and roughness affect cell proliferation. Cell density for osteoblasts grown on the indicated film types. $n = 6$ experiments.

cell adhesion was poorer in hydrophobic than wettable films, cell proliferation was comparable.

Hydrophobic materials with the appropriate microstructure and ability to self-hydrogenate may favor protein adsorption. It is generally acknowledged that proper material–protein adsorption may subsequently support cell proliferation and differentiation [15]. For example, osteoblastic cells' response to fibronectin-treated hydrophobic films lead to higher proliferation rates [16]. Thus, it is likely that hydrophobic films yielded good proliferation despite the initial adhesion being poor by capturing and later releasing growth factors present in the culture media.

The fact that specific physical and chemical attributes of SWNT films control different aspects of cell growth underscore the tremendous degree of flexibility of these materials. This is an important asset in view of the fact that they are biocompatible. By affording the possibility of maximizing a specific cellular response, initial attachment for instance, they might become versatile tools in multiple applications. We envision two specific areas of research that might benefit from these findings. One concerns the development of biomaterials that could facilitate bone-prosthesis attachment as well as bone-fracture healing, a problem quite common in the elderly. The second area concerns bioelectronic device development, that is, hybrid devices comprising living cells which are in operative contact with an extracellular planar potential-sensitive electrode, such as field effect transistors.

5. Conclusions

In summary, we have demonstrated that SWNT film properties alone can affect osteoblastic cell response. Our observations underscore a key role of φ and roughness in determining

initial cell attachment and proliferation. The best growing conditions were provided by medium rough ($R_q \sim 100$ nm) and hydrophilic samples with $\varphi \sim 45$ mJ m^{-2}.

References

[1] Hussain M A, Kabir M A and Sood A K 2009 On the cytotoxicity of carbon nanotubes *Curr. Sci.* **96** 664–73

[2] Khang D, Kim S Y, Liu-Snyder P, Palmore G T, Durbin S M and Webster T J 2007 Enhanced fibronectin adsorption on carbon nanotube/poly(carbonate) urethane: independent role of surface nano-roughness and associated surface energy *Biomaterials* **28** 4756–68

[3] Kam N W, O'Connell M, Wisdom J A and Dai H 2005 Carbon nanotubes as multifunctional biological transporters and near-infrared agents for selective cancer cell destruction *Proc. Natl Acad. Sci. USA* **102** 11600–5

[4] Singh R *et al* 2005 Binding and condensation of plasmid DNA onto functionalized carbon nanotubes: toward the construction of nanotube-based gene delivery vectors *J. Am. Chem. Soc.* **127** 4388–96

[5] Tutak W *et al* 2009 Toxicity induced enhanced extracellular matrix production in osteoblastic cells cultured on single-walled carbon nanotube networks *Nanotechnology* **20** 255101

[6] Hou P, Liu C and Cheng H 2008 Purification of carbon nanotubes *Carbon* **46** 2003–25

[7] Zheng L, Li Y and Liu J 2002 CVD synthesis and purification of single-walled carbon nanotubes on aerogel-supported catalyst *Appl. Phys.* A **74** 345–8

[8] Chen W, Li J, Liu L, Jia Z, Yu Y and Zhang Z 2003 Purification of carbon nanotubes using anodic oxidation in a solid polymer electrolyte (SPE) cell *J. Appl. Electrochem.* **33** 755–8

[9] Xu Y Q, Peng H, Hauge R H and Smalley R E 2005 Controlled multistep purification of single-walled carbon nanotubes *Nano Lett.* **5** 163–8

[10] Eda G, Fanchini G and Chhowalla M 2008 Bundling dynamics of single walled carbon nanotubes in aqueous suspensions *J. Appl. Phys.* **103** 093118

[11] Wu Z *et al* 2004 Transparent, conductive carbon nanotube films *Science* **305** 1273–6

[12] Parekh B B, Fanchini F, Eda G and Chhowalla M 2007 Improved conductivity of transparent single-wall carbon nanotube thin films via stable postdeposition functionalization *Appl. Phys. Lett.* **90** 121913

[13] Fanchini G, Unalan E H and Chhowalla M 2006 Optoelectronic properties of transparent and conducting single-wall carbon nanotube thin films *Appl. Phys. Lett.* **88** 191919

[14] Baier R E 1976 *Applied Chemistry at Protein Interfaces* (*Advances in Chemistry Series*) 1st edn (New York: American Chemical Society)

[15] Glasgow C K and Dhara D 2008 *Polymers for Biomedical Applications* 1st edn, ed A Mahapatro and S A Kulshrestha (Washington, DC: American Chemical Society)

[16] Kennedy S B, Washburn N R, Simon C G Jr and Amis E J 2006 Combinatorial screen of the effect of surface energy on fibronectin-mediated osteoblast adhesion, spreading and proliferation *Biomaterials* **27** 3817–24